Tetranuclear $[Mn^{III}Mn_3^{IV}O_4]$ Complexes as Spectroscopic Models of the S_2 State of the Oxygen Evolving Complex in Photosystem II

Heui Beom Lee[†], Angela A. Shiau[†], Paul H. Oyala[†], David Marchiori[‡], Sheraz Gul[§], Ruchira Chatterjee[§], Junko Yano[§], R. David Britt*[‡], and Theodor Agapie*[†]

† Department of Chemistry and Chemical Engineering, California Institute of Technology, 1200 E California Blvd MC 127-72, Pasadena, CA 91125, USA

‡ Department of Chemistry, University of California, Davis, Davis, California 95616, USA

§ Molecular Biophysics and Integrated Bioimaging Division, Lawrence Berkeley National Laboratory, Berkeley, CA 94720, USA

Supporting information

Experimental procedures

General considerations

All reactions were performed at room temperature in an N_2-filled glovebox or by using standard Schlenk techniques unless otherwise specified. Glassware was oven dried at 150ºC for at least 2h prior to use, and allowed to cool under vacuum. All reagents were used as received unless otherwise stated. Diphenylphosphinic acid was recrystallized from 95% ethanol. Tris(4-bromophenyl)aminium triflate was synthesized according to literature.[1] Anhydrous tetrahydrofuran (THF) was purchased from Aldrich in 18 L Pure-Pac^{TM} containers. Anhydrous CH_2Cl_2, CH_3CN, diethyl ether, benzene and THF were purified by sparging with nitrogen for 15 minutes and then passing under nitrogen pressure through a column of activated A2 alumina. NMR solvents were purchased from Cambridge Isotope Laboratories, dried over calcium hydride, degassed by three freeze-pump-thaw cycles and vacuum-transferred prior to use. ^{1}H NMR spectra were recorded on a Varian 300 MHz instrument, with shifts reported relative to the residual solvent peak. Elemental analyses were performed at the California Institute of Technology.

Synthesis of propane-1,3-diacetamide (H_2diam)

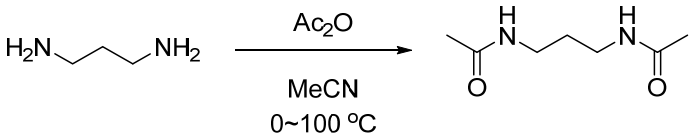

(*Caution! 1,3-diaminopropane fumes in air and is very toxic!*) A round bottom flask equipped with a magnetic stir bar was charged with a solution of 1,3-diaminopropane (19 mL) in MeCN (200 mL) and cooled in an ice bath. Three equivalents of acetic anhydride (65 mL) were added dropwise via an addition funnel. Immediately, an exothermic reaction ensued. While a white precipitate was observed initially, a homogeneous, colorless solution was obtained as the reaction progressed. Upon complete addition of acetic anhydride, the temperature was raised to 100 ºC and all volatiles were distilled off under partial vacuum, leaving behind a white, crystalline residue. This residue was washed with Et_2O, air-dried, crushed into a fine powder using a mortar and pestle, and washed once again with Et_2O. Propane-1,3-diacetamide was isolated as a white powder. ^{1}H NMR (300 MHz, DMSO−d^6) 7.812 (bs, 2H), 3.01 (td, J = 7.0, 5.6 Hz, 4H), 1.78 (s, 6H), 1.49 (p, J = 7.1 Hz, 2H).

Synthesis of **2-ox**

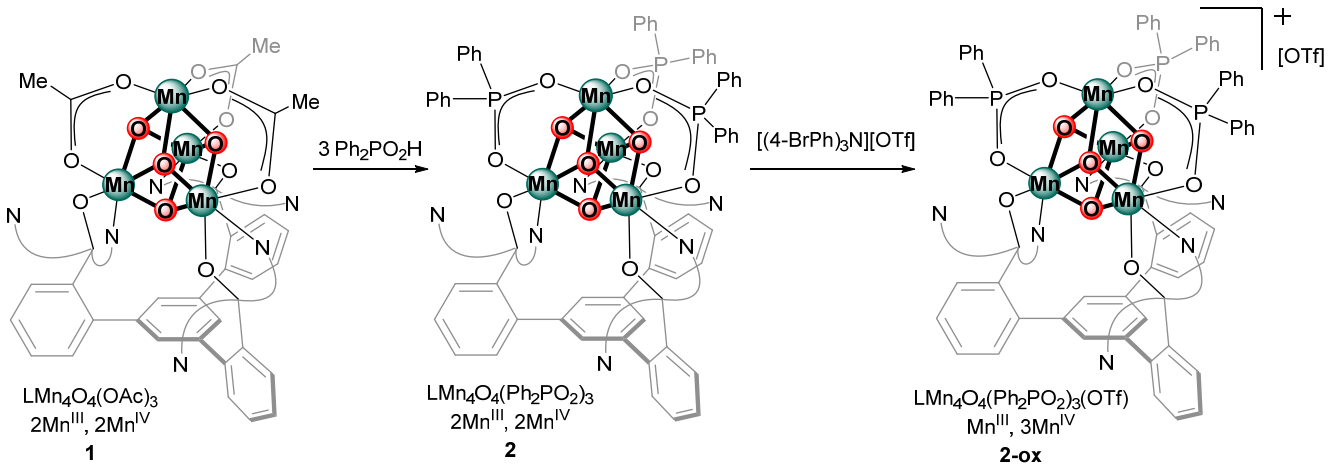

A solution of $LMn_4O_4(OAc)_3$ (600 mg, 0.46 mmol, 1 equiv) in CH_2Cl_2 (12 mL) was added to a stirring CH_2Cl_2 suspension of diphenylphosphinic acid (330 mg, 1.51 mmol, 3.3 equiv). After stirring the reaction at room temperature for 16 hours, a colorless precipitate formed and was filtered away. All volatiles were removed from the filtrate under reduced pressure. The solid residue was triturated with CH_2Cl_2 (15 mL) and Et_2O (15 mL). The brown powder was then suspended in 15 mL of THF, collected on a pad of Celite, dissolved in CH_2Cl_2, and filtered through Celite. All volatiles were removed from the filtrate under reduced pressure, yielding compound **2** as a red-brown powder. Yield = 462 mg, 57 %. Crystals suitable for X-ray crystallography were grown from slow vapor diffusion of Et_2O into a concentrated solution of **2** in CH_2Cl_2.

To a stirring solution of **2** (150 mg, 84 µmol, 1 equiv) in CH_2Cl_2 (5 mL), a blue CH_2Cl_2 solution (4 mL) of $[(4\text{-}BrPh)_3N][OTf]$ (53 mg, 84 µmol, 1 equiv) was added. After the brown solution was stirred at room temperature for 16 hours, all volatiles were removed under reduced pressure. The residue was washed with Et_2O (4 mL), washed with THF until the filtrate was no longer blue/green, dissolved in CH_2Cl_2, and filtered through Celite. Volatiles were removed from the filtrate under reduced pressure, yielding **2-ox** as a brown powder (112 mg, 69 %). Crystals suitable for X-ray crystallography were obtained from a slow vapor diffusion of Et_2O into a concentrated solution of **2-ox** in CH_2Cl_2. Analysis calculated for $LMn_4O_4(O_2PPh_2)_3(OTf)$ $[C_{94}H_{69}F_3Mn_4N_6O_{16}P_3S]$: C 58.19, H 3.58, N 4.33; found: C 58.00, H 3.79, N 4.66.

Synthesis of **3-ox**

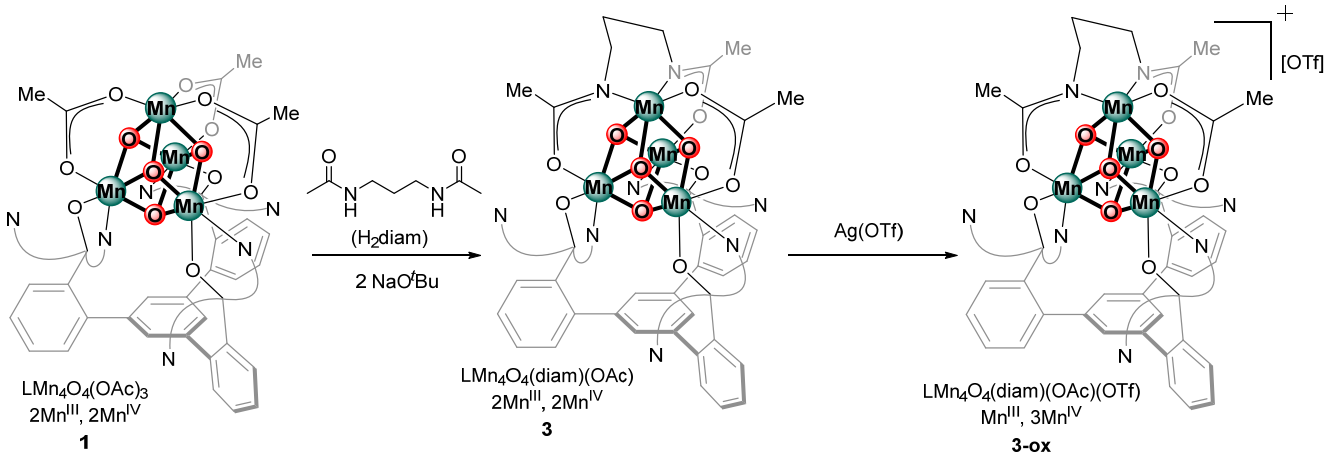

To a stirred suspension of $LCaMn_3O_4(OAc)_3(THF)$ (660 mg, 0.5 mmol, 1 equiv) in DMF (10 mL) was added $Mn(OTf)_2$•2MeCN (230 mg, 0.53 mmol, 1.06 equiv) and propane-1,3-diacetamide (84 mg, 0.53 mmol, 1.06 equiv). After stirring the reaction mixture at room temperature for 1 hour, sodium *tert*-butoxide (102 mg, 1.06 mmol, 2.1 equiv) was added and additional DMF was added to adjust the volume of the reaction to 20 mL. After stirring at room temperature for 18 hours, the precipitate formed in the reaction mixture was collected on a pad of Celite. The precipitate was rinsed with additional DMF and subsequently with Et_2O. The solid residue was dissolved in CH_2Cl_2 and filtered through Celite. All volatiles were removed from the filtrate under reduced pressure. Compound **3** was isolated as air- and moisture-stable red powder. Yield = 330 mg, 50 %. Crystals suitable for X-ray crystallography were obtained by slow vapor diffusion of Et_2O into a concentrated solution of **3** in CH_2Cl_2. Analysis calculated for LMn_4O_4(diamidate)$(OAc)\cdot\frac{1}{2}CH_2Cl_2\cdot Et_2O$ [$C_{71}H_{65}ClMn_4N_8O_{12}$]: C 57.72, H 4.43, N 7.58; found (duplicate runs): C 57.68, H 4.77, N 7.28; C 57.70, H 4.74, N 7.23.

To a suspension of **3** (70 mg, 52 µmol, 1 equiv) in THF (10 mL), Ag(OTf) (15 mg, 58 µmol, 1.1 equiv) was added as a THF solution. After stirring for 18 hrs, the reaction mixture was filtered through a pad of Celite and concentrated under reduced pressure. The residue was washed with generous amounts of Et_2O, redissolved in CH_2Cl_2, and filtered through a pad of Celite. All volatiles were removed from the filtrate under reduced pressure. Crystals suitable for X-ray crystallography were obtained by slow vapor diffusion of Et_2O into a concentrated solution of **3-ox** in CH_2Cl_2. Yield = 30 mg, 39 %. Analysis calculated for LMn_4O_4(diamidate)$(OAc)(OTf)\cdot CH_2Cl_2$ [$C_{68}H_{56}Cl_2F_3Mn_4N_8O_{14}S$]: C 51.40, H 3.55, N 7.05; found (duplicate runs): C 51.26, H 3.49, N 6.73; C 51.24, H 3.61, N 6.87.

Synthesis of **4-ox**

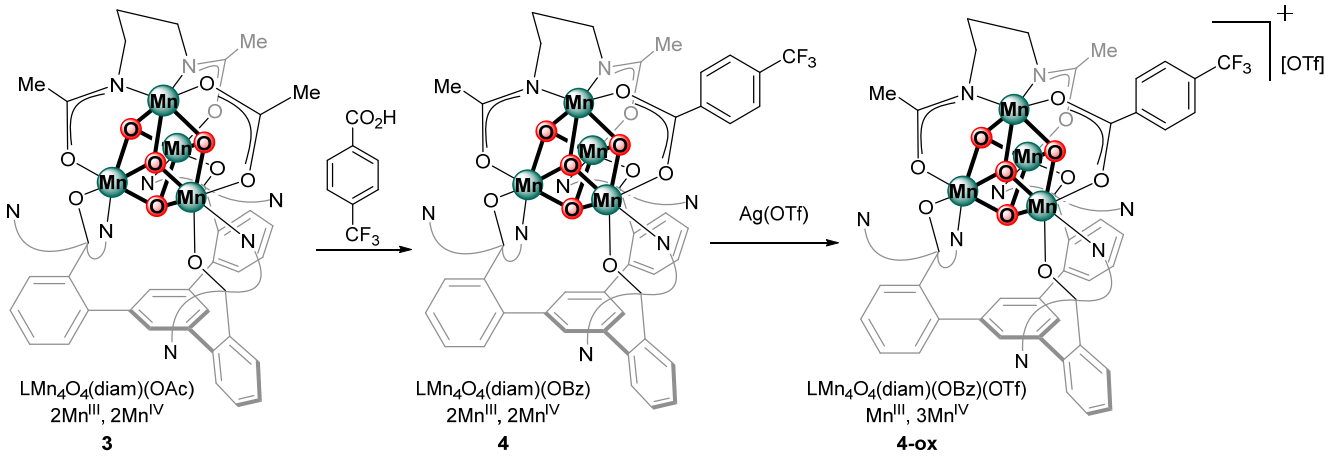

To a stirred solution of **3** (282 mg, 0.21 mmol, 1 equiv) in CH_2Cl_2 (10 mL) was added a solution of *p*-CF_3-benzoic acid (50 mg, 0.26 mmol, 1.25 equiv) in THF (5 mL). After stirring the resulting red solution at room temperature for 6 hours, all volatiles were removed under reduced pressure. To ensure complete substitution, the residue was redissolved in THF, stirred for 1 hour, and all volatiles removed under reduced pressure. This procedure was repeated three times. The solid residue was rinsed with hexanes and subsequently with diethyl ether. The solid residue was dissolved in benzene and filtered through Celite. All volatiles were removed from the filtrate under reduced pressure. The residue was rinsed with MeCN and subsequently with diethyl ether, and dried under reduced pressure. Compound **4** was isolated as a red powder. Yield = 260 mg, 84 %. Crystals suitable for X-ray crystallography could not be obtained.

To a stirred solution of **4** (230 mg, 0.15 µmol, 1 equiv) in CH_2Cl_2 (5 mL), a solution of Ag(OTf) (42 mg, 0.16 µmol, 1.1 equiv) in THF (5 mL) was added. After stirring the resulting mixture at room temperature for 18 hours, the reaction mixture was filtered through a pad of Celite and concentrated under reduced pressure. The residue was washed with a generous amount of Et_2O, redissolved in benzene, and filtered through a pad of Celite. All volatiles were removed from the filtrate under reduced pressure. Crystals suitable for X-ray crystallography were obtained by slow vapor diffusion of Et_2O into a concentrated solution of **4-ox** in CH_2Cl_2. Yield = 147 mg, 58 %. Analysis calculated for LMn_4O_4(diamidate)(OBz)(OTf)·CH_2Cl_2 [$C_{74}H_{57}Cl_2F_6Mn_4N_8O_{14}S$]: C 51.70, H 3.34, N 6.52; found: C 51.51, H 3.38, N 6.76.

NMR spectroscopy

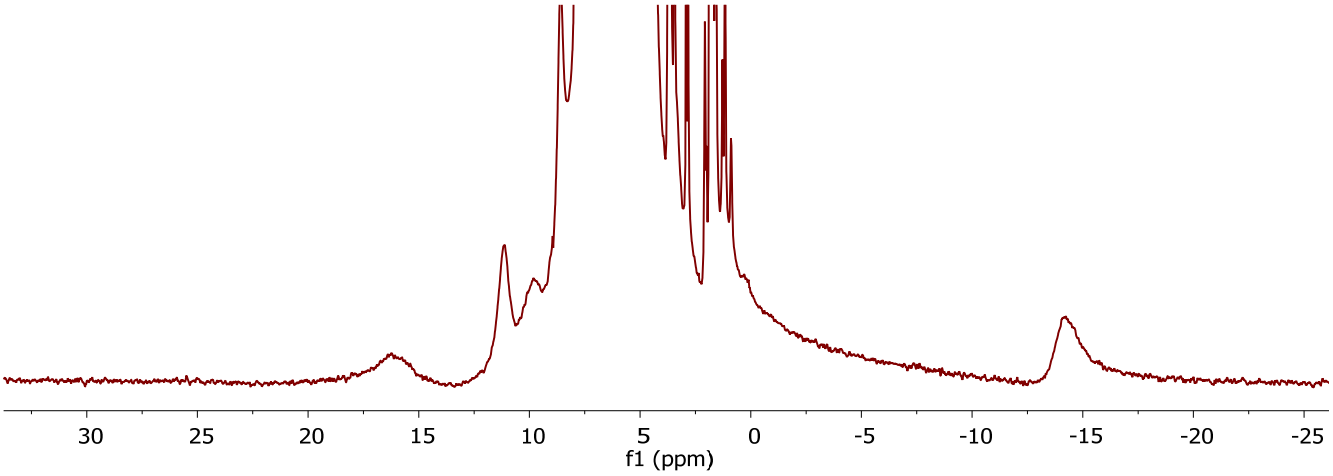

Figure S1. ^{1}H NMR of **2** in CD_2Cl_2.

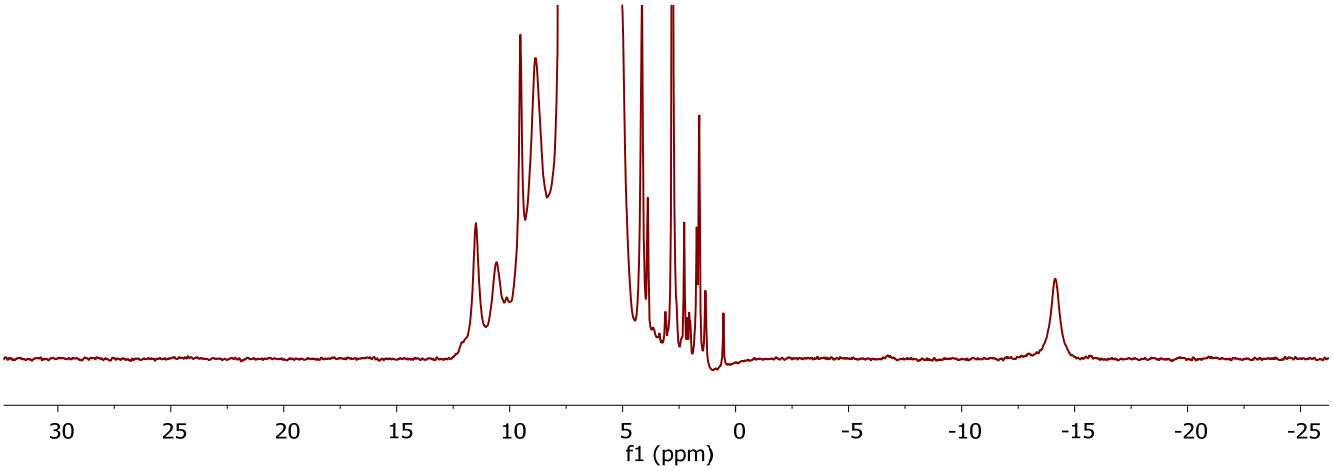

Figure S2. ^{1}H NMR of **2-ox** in CD_2Cl_2.

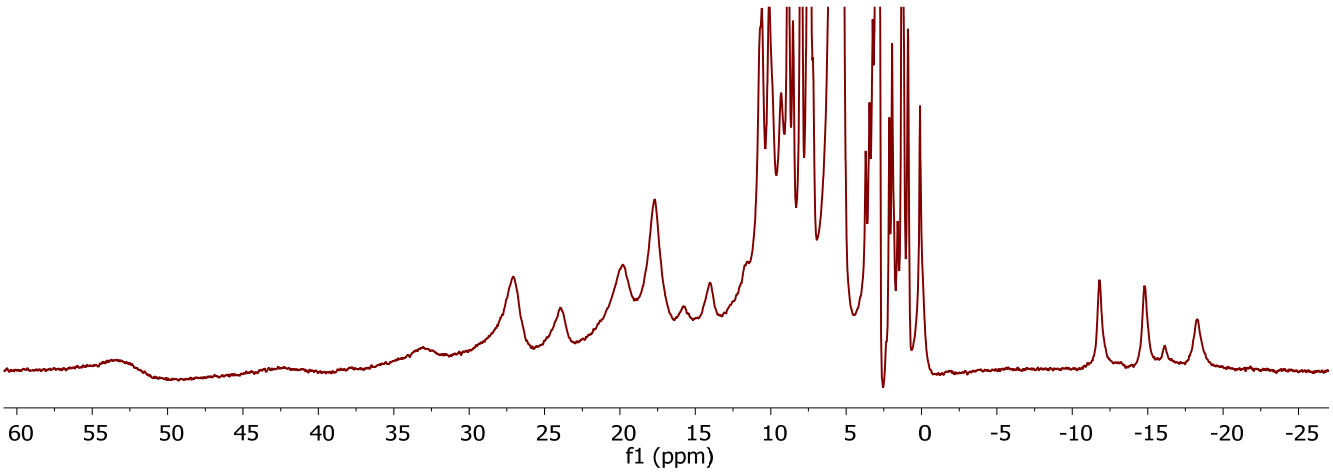

Figure S3. ^{1}H NMR of **3** in CD_2Cl_2.

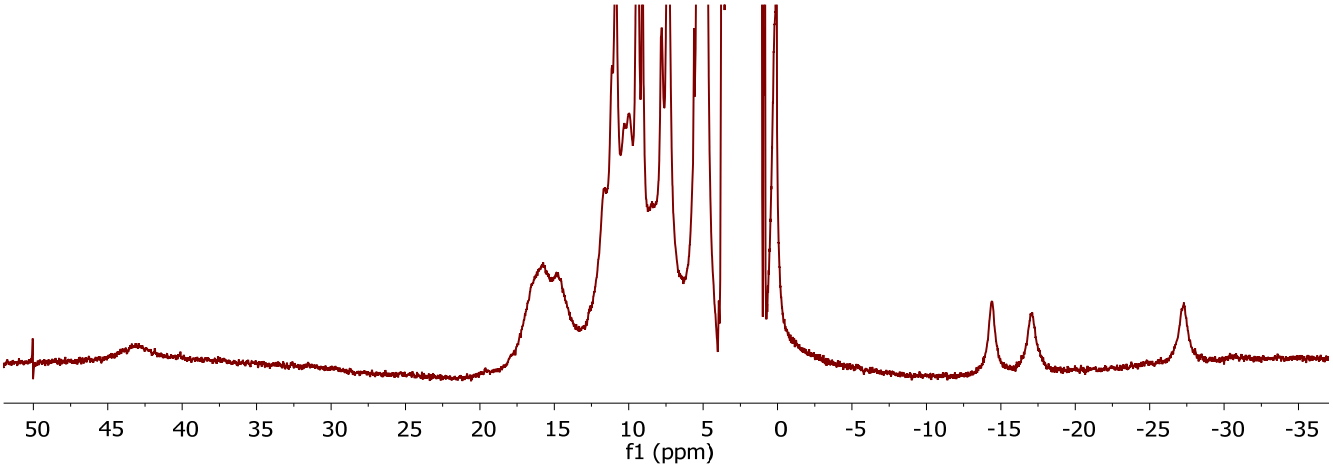

Figure S4. ^{1}H NMR of **3-ox** in CD_2Cl_2.

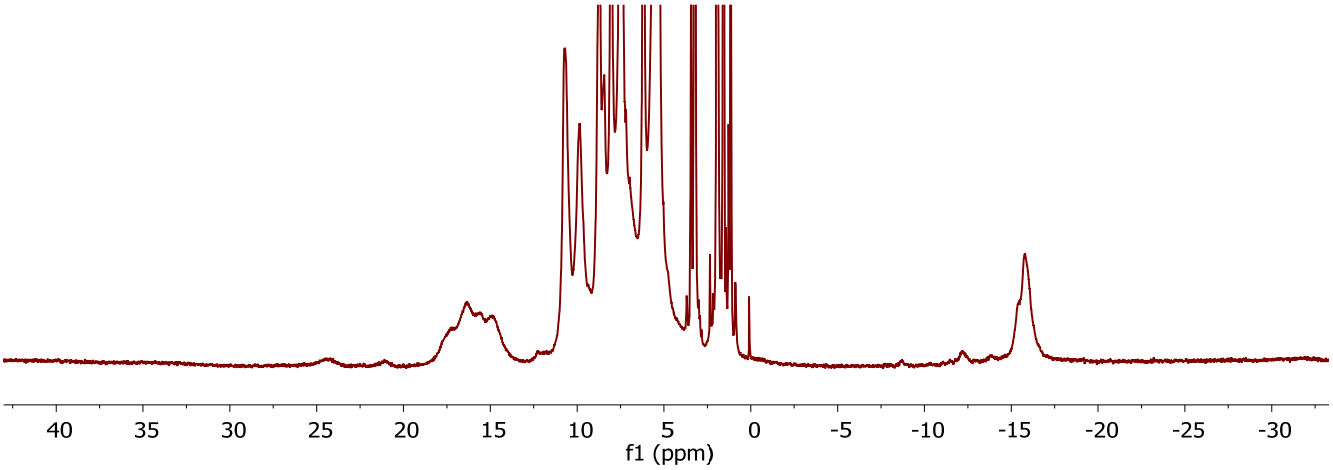

Figure S5. ^{1}H NMR of **4** in CD_2Cl_2.

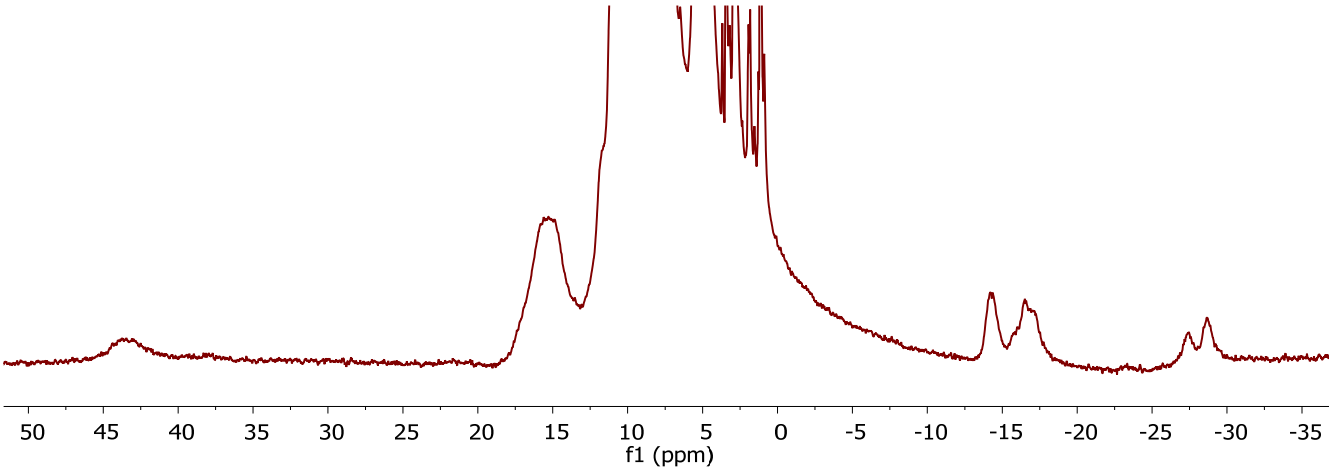

Figure S6. ^{1}H NMR of **4-ox** in CD_2Cl_2.

ESI-MS spectrometry

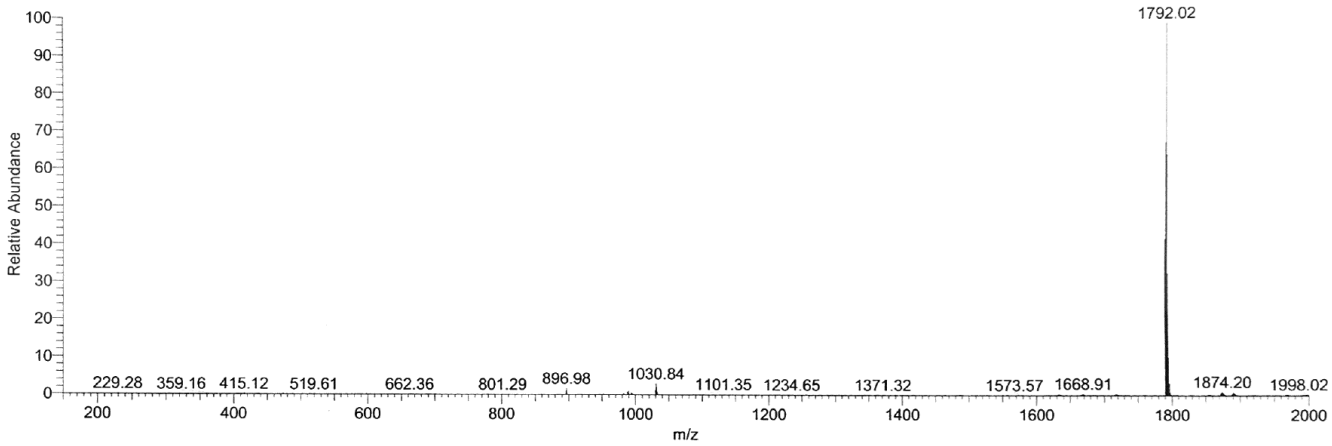

Figure S7. ESI-MS of **2**. m/z = 1792 consistent with $[LMn_4O_4(O_2PPh_2)_3]^+$.

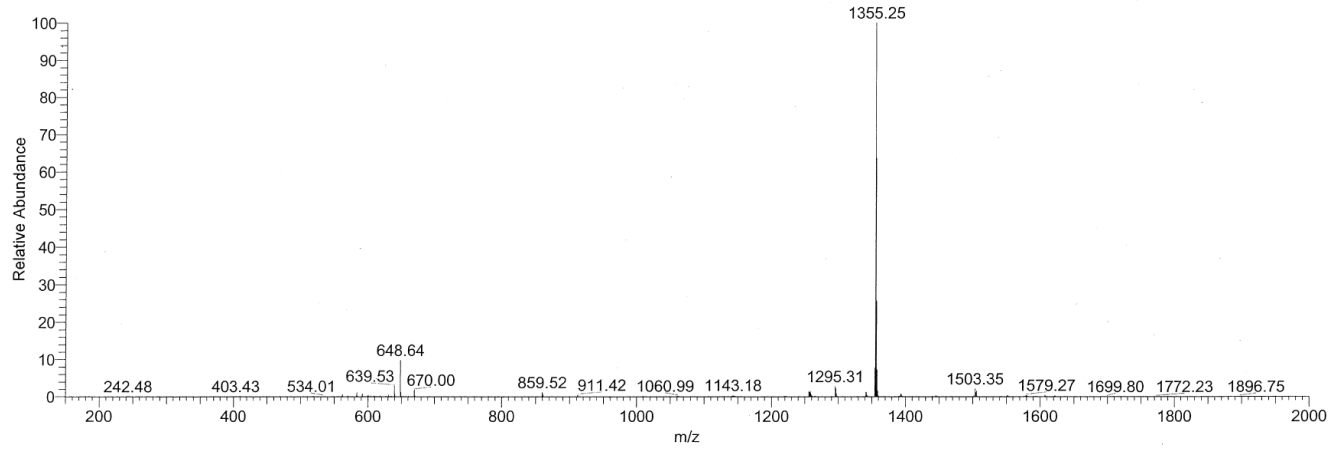

Figure S8. ESI-MS of **3**. m/z = 1355 consistent with $[LMn_4O_4(diam)(OAc)]^+$.

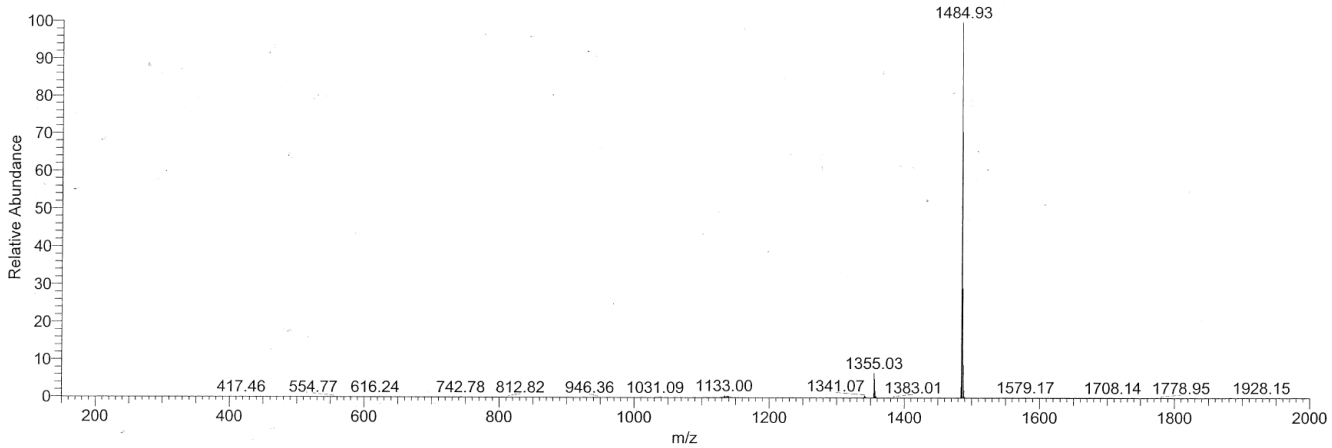

Figure S9. ESI-MS of **4-ox**. m/z = 1485 consistent with $[LMn_4O_4(diam)(OBz)]^+$.

X-ray crystallography

Suitable crystals were mounted on a nylon loop using Paratone oil, then placed on a diffractometer under a nitrogen stream. X-ray intensity data were collected on a Bruker D8 VENTURE Kappa Duo PHOTON 100 CMOS detector employing Mo-Kα or Cu-Kα radiation (λ = 0.71073 Å or 1.54178 Å respectively) at a temperature of 100 K. All diffractometer manipulations, including data collection, integration and scaling were carried out using the Bruker APEX3 software. Frames were integrated using SAINT. The intensity data were corrected for Lorentz and polarization effects and for absorption using SADABS. Space groups were determined on the basis of systematic absences and intensity statistics using XPREP. Using Olex2, the structures were solved by direct methods using ShelXT and refined to convergence by full-matrix least squares minimization using ShelXL. All non-solvent non-hydrogen atoms were refined using anisotropic displacement parameters. Hydrogen atoms were placed in idealized positions and refined using a riding model. Graphical representation of structures with 50% probability thermal ellipsoids was generated using Diamond visualization software. No special refinement details.

Table S1. Crystal and refinement data for complexes **2**, **2-ox**, and **3**.

Compound	**2**	**2-ox**	**3**
CCDC	1863637	1863638	1863639
Empirical formula	$C_{94}H_{71}Cl_2Mn_4N_6O_{13}P_3$	$C_{95}H_{71}Cl_2F_3Mn_4N_6O_{16}P_3S$	$C_{73.55}H_{56}Cl_{2.51}Mn_4N_8O_{12.57}$
Formula weight	1876.13	2025.20	1561.80
Temperature/K	296.15	100.0	100.0
Crystal system	triclinic	monoclinic	triclinic
Space group	P-1	$P2_1/n$	P-1
a/Å	14.2765(10)	14.3608(9)	13.2586(18)
b/Å	14.3034(8)	27.4932(17)	15.443(3)
c/Å	23.7048(18)	23.6617(14)	18.255(3)
α/°	72.614(2)	90	89.004(5)
β/°	87.529(2)	101.255(2)	85.374(5)
γ/°	67.645(2)	90	82.474(5)
Volume/Å^3	4258.6(5)	9162.5(10)	3693.5(10)
Z	2	4	2
ρ_{calc}g/cm^3	1.463	1.468	1.404
μ/mm^{-1}	0.767	0.748	0.825
F(000)	1920.0	4132.0	1593.0
Crystal size/mm^3	0.1 × 0.1 × 0.1	0.1 × 0.05 × 0.03	0.1 × 0.1 × 0.1
Radiation	MoKα (λ = 0.71073)	MoKα (λ = 0.71073)	MoKα (λ = 0.71073)
2Θ range for data collection/°	3.094 to 61.002	4.272 to 72.664	4.992 to 61.126
Index ranges	-20 ≤ h ≤ 19, -20 ≤ k ≤ 20, -33 ≤ l ≤ 33	-23 ≤ h ≤ 23, -45 ≤ k ≤ 45, -39 ≤ l ≤ 39	-18 ≤ h ≤ 18, -22 ≤ k ≤ 22, -26 ≤ l ≤ 26
Reflections collected	163138	470337	130778
Independent reflections	25775 [R_{int} = 0.0594, R_{sigma} = 0.0494]	43739 [R_{int} = 0.0541, R_{sigma} = 0.0346]	22581 [R_{int} = 0.0305, R_{sigma} = 0.0250]
Data/restraints/parameters	25775/0/1099	43739/30/1211	22581/37/935
Goodness-of-fit on F^2	1.012	1.049	1.052
Final R indexes [I>=2σ (I)]	R_1 = 0.0495, wR_2 = 0.1122	R_1 = 0.0590, wR_2 = 0.1539	R_1 = 0.0626, wR_2 = 0.1885
Final R indexes [all data]	R_1 = 0.0780, wR_2 = 0.1244	R_1 = 0.0861, wR_2 = 0.1739	R_1 = 0.0781, wR_2 = 0.2028
Largest diff. peak/hole / e Å^{-3}	0.90/-1.32	2.16/-2.32	2.25/-1.47

Table S2. Crystal and refinement data for complexes **3-ox**, and **4-ox**.

Compound	**3-ox**	**4-ox**
CCDC	1863640	1863641
Empirical formula	$C_{68}H_{57}Cl_2F_3Mn_4N_8O_{14}S$	$C_{77}H_{65}F_6Mn_4N_8O_{15}S$
Formula weight	1589.93	1708.19
Temperature/K	100.04	99.99
Crystal system	triclinic	monoclinic
Space group	P-1	C2/c
a/Å	12.925(2)	41.9795(15)
b/Å	15.479(2)	15.5642(8)
c/Å	18.467(3)	26.7105(8)
α/°	81.151(6)	90
β/°	84.367(6)	122.4230(10)
γ/°	66.925(7)	90
Volume/$Å^3$	3355.5(9)	14731.5(10)
Z	2	8
$\rho_{calc}g/cm^3$	1.574	1.540
μ/mm^{-1}	7.697	0.787
F(000)	1620.0	6984.0
Crystal size/mm^3	0.02 × 0.02 × 0.02	0.1 × 0.1 × 0.05
Radiation	CuKα (λ = 1.54178)	MoKα (λ = 0.71073)
2Θ range for data collection/°	6.256 to 150.802	4.328 to 61.122
Index ranges	$-16 \le h \le 15$, $-19 \le k \le 19$, $-23 \le l \le 23$	$-59 \le h \le 59$, $-22 \le k \le 22$, $-38 \le l \le 38$
Reflections collected	51382	150607
Independent reflections	13628 [R_{int} = 0.0684, R_{sigma} = 0.0600]	22494 [R_{int} = 0.0436, R_{sigma} = 0.0305]
Data/restraints/parameters	13628/0/914	22494/0/1004
Goodness-of-fit on F^2	1.029	1.051
Final R indexes [I>=2σ (I)]	R_1 = 0.0786, wR_2 = 0.2145	R_1 = 0.0766, wR_2 = 0.2334
Final R indexes [all data]	R_1 = 0.1078, wR_2 = 0.2416	R_1 = 0.0991, wR_2 = 0.2585
Largest diff. peak/hole / e $Å^{-3}$	3.12/-1.56	2.58/-2.61

Electrochemistry

Measurements were performed under an inert N_2 atmosphere in the glovebox using a Pine Instrument Company AFCBP1 bipotentiostat using the AfterMath software package. Cyclic voltammograms were recorded on 1.0 mM solutions of the relevant complex in the glovebox at 20 °C with an auxiliary Pt-coil counter electrode, Ag-wire reference electrode, and 3.0 mm glassy carbon working electrode (BASI). The electrolyte solution was 0.1 M [^{n}Bu$_4$N][PF$_6$] in propylene carbonate. All reported values are referenced to an internal ferrocene/ferrocenium couple. Square-wave voltammograms were recorded using the following experimental parameters: amplitude 0.1 V, period 1 s, increment 10 mV, sampling width 1 ms.

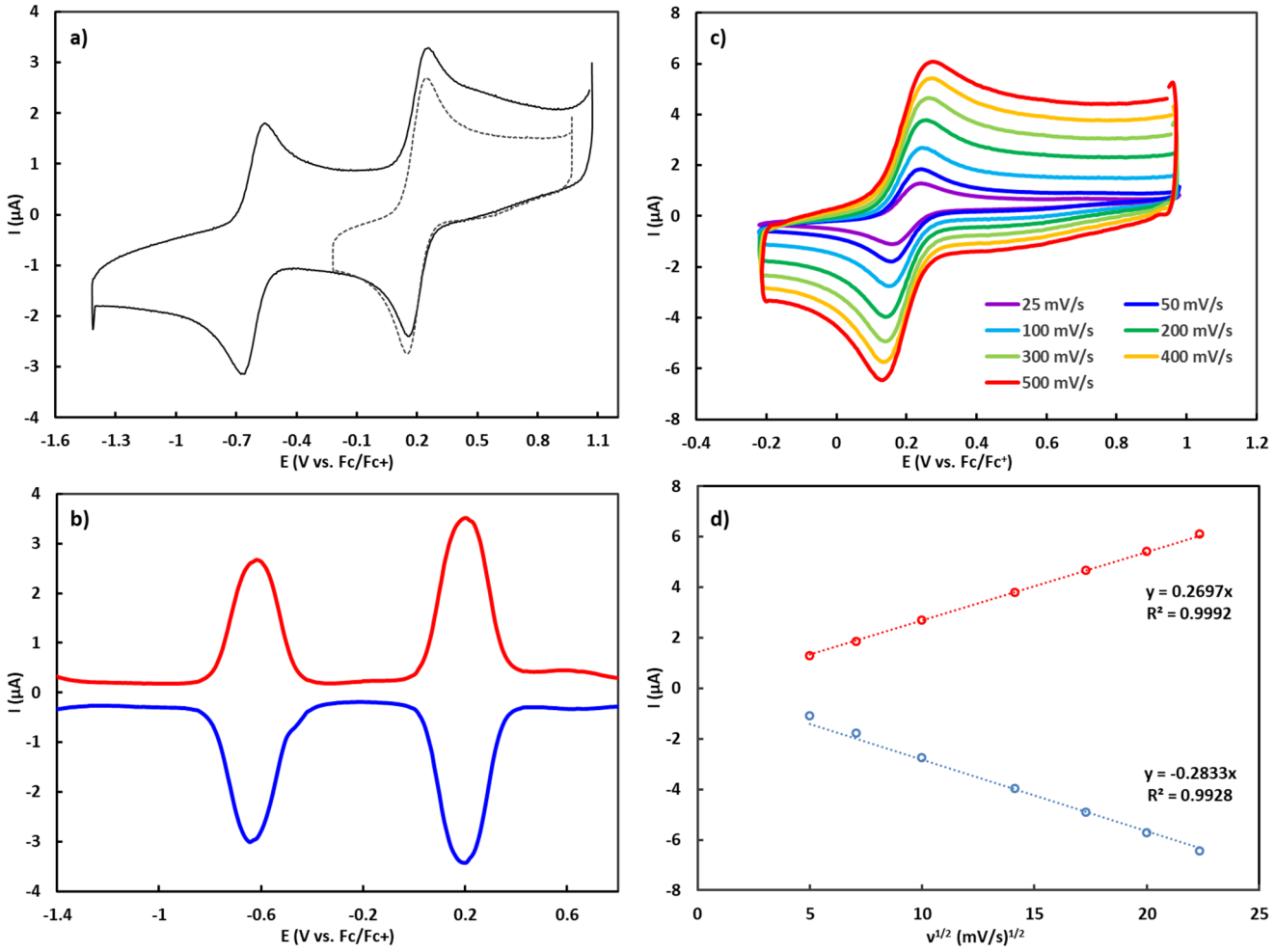

Figure S10. a) CV of **2**. Isolated redox couple shown in dotted lines. E = + 194 mV vs. Fc/Fc$^+$. b) SWV of **2**. c) Isolated redox couple measured at various scan rates. d) Plot of peak current vs. square root of scan rate.

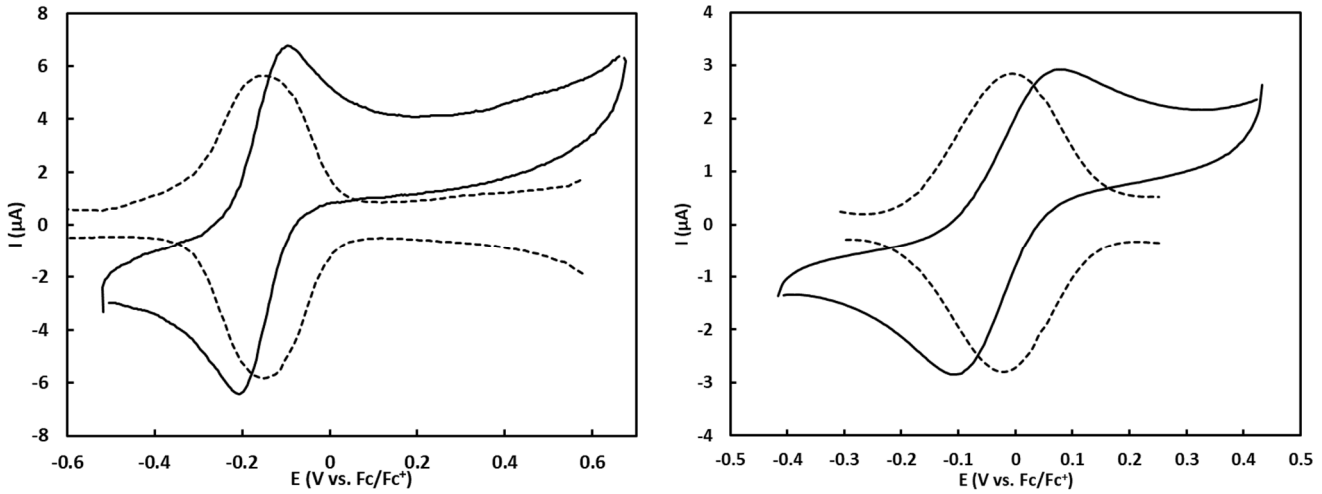

Figure S11. (Left) CV (solid lines) and SVW (dotted lines) of **3** in propylene carbonate. E = −150 mV vs. Fc/Fc^+. (Right) CV (solid lines) and SVW (dotted lines) of **4** in propylene carbonate. E = −15 mV vs. Fc/Fc^+.

X-ray Absorption Spectroscopy (XAS)

Mn K-edge X-ray absorption data were collected using bemline 9-3 at Stanford Sychrotron Radiation Laboratory (SSRL) operating with standard ring conditions of 3.0 GeV energy and 500 mA current. A Si (220) double crystal monochromator detuned to 50% of flux maximum at Mn K-edge was used to minimize the higher harmonics. A harmonic rejection mirror was used to further reduce the contamination of higher harmonics. The intensities of incident and transmitted X-rays were monitored with N_2-filled ion chambers before the sample (I_0) and after the sample (I_1 and I_2), respectively. The solid samples were packed in 0.5 mm thick aluminum sample holders and sealed with Kapton tape windows on both sides. For liquid samples, ~10 mM solutions of samples in dimethylformamide were loaded in 40 µL plexiglass sample holders having Mylar tape window on one side, and frozen immediately in liquid nitrogen. XAS data of samples were collected as fluorescence excitation spectra using a 30-element Ge solid-state detector (Canberra). The monochromator energy was calibrated with the pre-edge peak of $KMnO_4$ (6543.3 eV). $KMnO_4$ calibration standard was placed between the N_2-filled ion chambers (I_1 and I_2) after the sample and its Mn spectra were simultaneously recorded along with samples for internal energy calibration. To minimize the X-ray damage, data was collected at 10 K using a liquid He flow cryostat (Oxford Instruments). The XAS scans of samples were closely monitored for any X-ray induced damage during the course of measurements.

Data reduction of XAS spectra was performed using SamView (SixPack software, available at http://www.sams-xrays.com/sixpack). Athena program of Demeter software package (Demeter version 0.9.26, B. Ravel)[2] was used to align/merge XAS data and subtract the pre-edge and post-edge backgrounds. The spectra were then normalized to the edge jump. A five-domain cubic spline was used to remove the low frequency background in *k*-space and resulting *k*-space data, $k^3\chi(k)$, was then Fourier transformed (FT) into *r*-space. Fitting of the EXAFS data was performed in *r*-space with Artemis software (Demeter version 0.9.26, B. Ravel) using *ab initio* phases and amplitudes calculated with the program FEFF6[3] and crystal structure data.

During the curve fitting process, coordination number (N) was fixed while the bond distance between the absorber and scattering atoms (R), and mean square displacement of the bond distance (σ^2) were allowed to vary. The non-structural parameter E_0 (which defines the zero value energy of the photoelectron wave vector *k*) was also used as a variable but restricted to a common value for each path in a given fit. The value for the passive electron reduction factor (S_0^2) was determined from the fit to the data of $KMnO_4$, and was fixed during the fits (0.85).

Fourier Transforms of k^3-weighted Mn EXAFS data for complexes **2-ox**, **3-ox** and **4-ox** in solid phase are shown in Figure S12 along with the corresponding best fits. It is important to note that the x-axis represents the non-phase-shift corrected radial distance (R') which is shorter than the actual scatterer distance by ~0.5 Å originating from the phase shift. The first peak in the FT data corresponds to metal-ligand (Mn-O/N) scattering whereas second peak includes metal-metal/metal-ligand interactions (Mn-Mn, Mn-C/P). The scattering contribution from relatively heavier P atoms results in greater amplitude of second peak in the EXAFS data of complex **2-ox** as compared to **3-ox** and **4-ox**. For each complex two metal-ligand distances were used for the first peak to get the best fit. In case of complex **2-ox**, one of the Mn atoms has three P second neighbors whereas each of the other three Mn has only one P second neighbor. Therefore, an average coordination number of 1.50 was used to fit the data. Similarly, an average coordination number (2.25) was used for C atoms contributing to the second shell as each of the three Mn atoms with one P in second shell is linked to three C atoms. The best fit parameters obtained are listed in Table S3. The bond distances extracted from fits to the EXAFS data are in good agreement with those determined from XRD data.

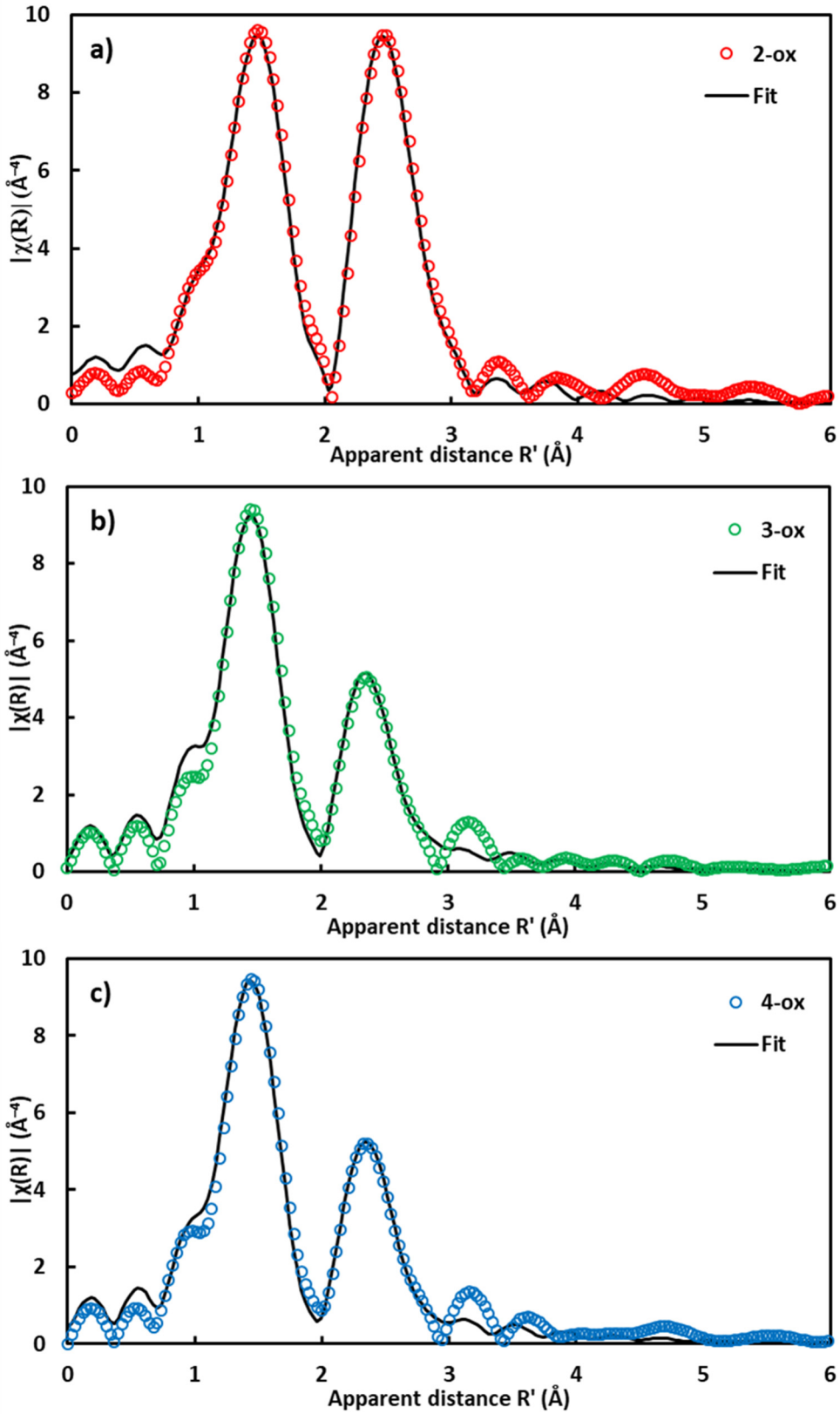

Figure S12 Fourier Transforms of k^3-weighted Mn K-edge EXAFS data (circles) along with the respective best fits (black line) for complexes **2-ox** (a), **3-ox** (b) and **4-ox** (c). The corresponding best fit parameters are presented in Table S3.

Table S3: Best fit parameters for Mn K-edge EXAFS curve fitting of complexes **2-ox**, **3-ox** and **4-ox**.[a]

Sample	Path	R (Å)		N	σ^2 (10^{-3} Å^2)	R-factor (%)	ΔE_0 (eV)
		EXAFS	XRD				
2-ox	Mn-O	1.83±0.01	1.83-1.91	3	5.50±1.05	0.80	-0.51±0.94
	Mn-O/N	1.93±0.01	1.92-2.24	3	2.00±0.20		
	Mn-Mn	2.86±0.01	2.85-2.96	3	4.23±0.94		
	Mn-C	2.96±0.01	2.77-3.05	2.25	2.00±0.61		
	Mn-P	3.08±0.01	3.07-3.15	1.50	2.00±0.81		
3-ox	Mn-O	1.81±0.02	1.83-1.92	3	8.00±1.52	1.96	-5.00±3.50
	Mn-O/N	1.91±0.02	1.93-2.06	3	2.00±0.20		
	Mn-Mn	2.79±0.02	2.76-2.96	3	6.15±2.24		
	Mn-C	3.01±0.10	2.79-3.04	4	6.04±6.99		
4-ox	Mn-O	1.82±0.02	1.83-1.92	3	5.01±2.25	1.21	-3.57±2.63
	Mn-O/N	1.92±0.02	1.93-2.08	3	2.00±0.20		
	Mn-Mn	2.79±0.01	2.75-2.99	3	5.58±2.17		
	Mn-C	2.98±0.06	2.79-3.05	4	5.27±5.28		

[a] EXAFS data for complex **2-ox** was fit in the k-range $2.84 \leq k(Å^{-1}) \leq 10.79$ ($1.0 \leq R'(Å) \leq 3.2$). EXAFS data of complex **3-ox** was fit in the k-range $2.79 \leq k(Å^{-1}) \leq 11.30$ ($1.0 \leq R'(Å) \leq 2.9$). EXAFS data for complex **4-ox** was fit in the k-range $2.79 \leq k(Å^{-1}) \leq 11.21$ ($1.0 \leq R'(Å) \leq 2.9$).

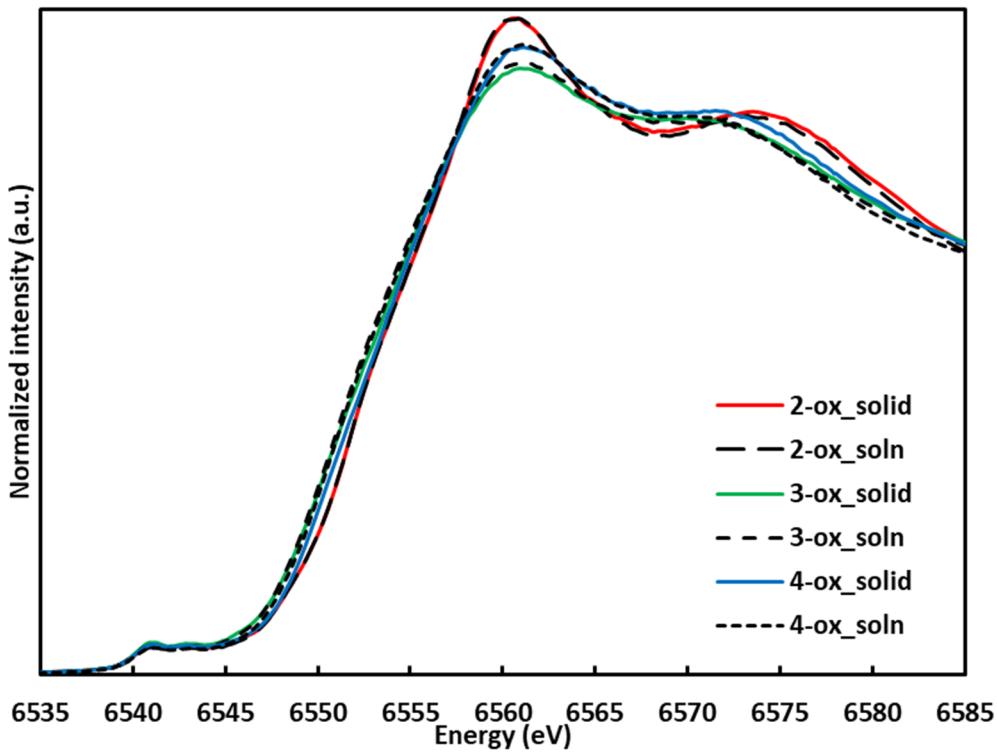

Figure S13 Normalized XANES data at Mn *K*-edge for complexes **2-ox**, **3-ox**, and **4-ox** in solid and solution phases.

SQUID magnetometry

Magnetic susceptibility measurements were carried on a Quantum Design MPMS 3 instrument running MPMS Multivu software. Crystalline samples were powdered and suspended in clear plastic straws in polycarbonate capsules. Data were recorded at 0.4 T from 1.8−300 K. Diamagnetic corrections were made as follows: –970, –795, and –860 × 10^{-6} cm^3/mol for **2-ox**, **3-ox**, and **4-ox**, respectively. Fitting simulations were performed using PHI.[4] Fitting simulations were performed assuming an on-site zero field splitting parameter $D(Mn^{IV}) \approx 0$ cm^{-1} and $D(Mn^{III}) = 0$, −2, or −4 cm^{-1}. The average *J* values are reported along with the standard deviation.

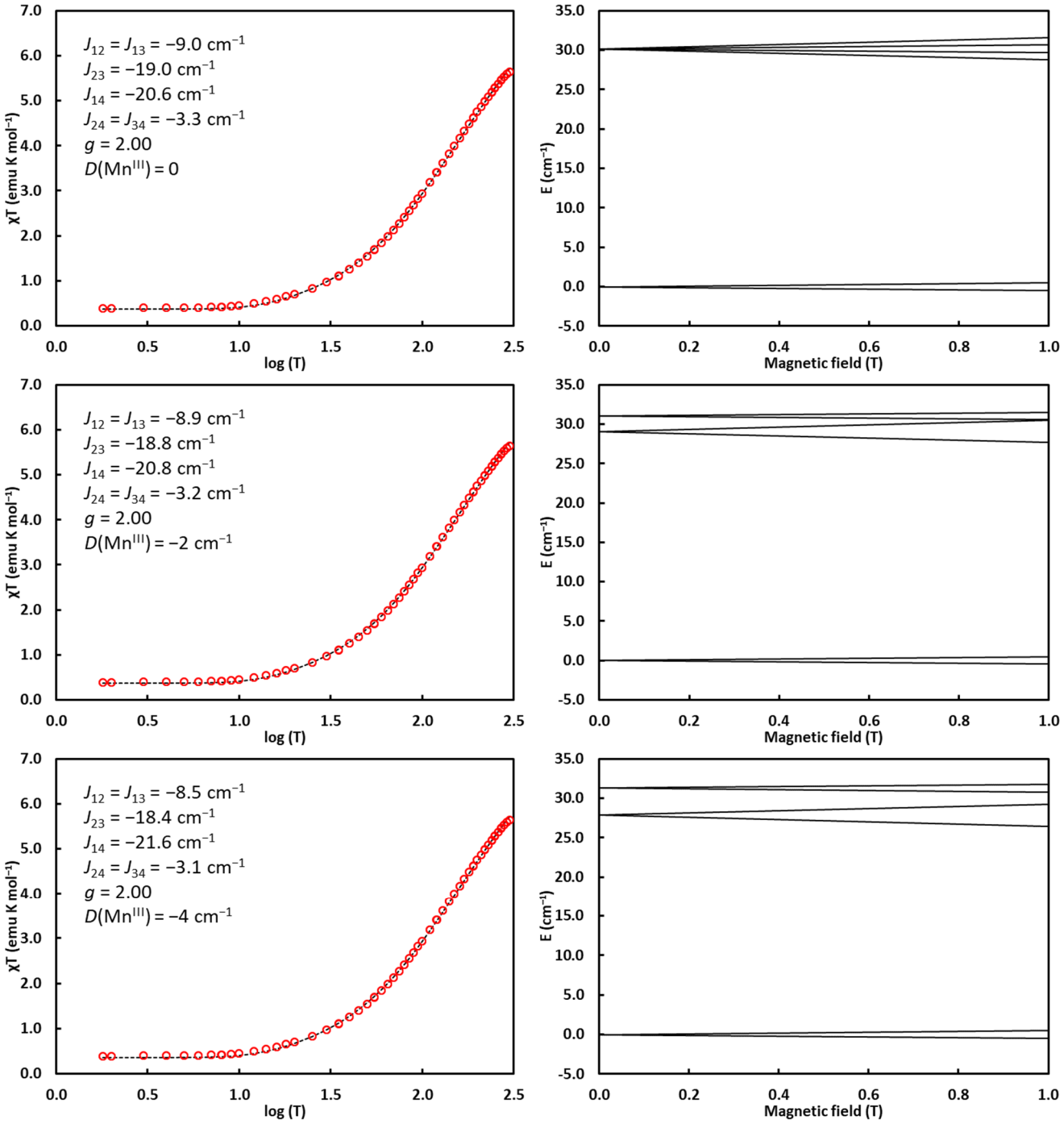

Figure S14. Fit parameters and corresponding χT vs. log(T) plots and Zeeman splitting diagrams for **2-ox**.

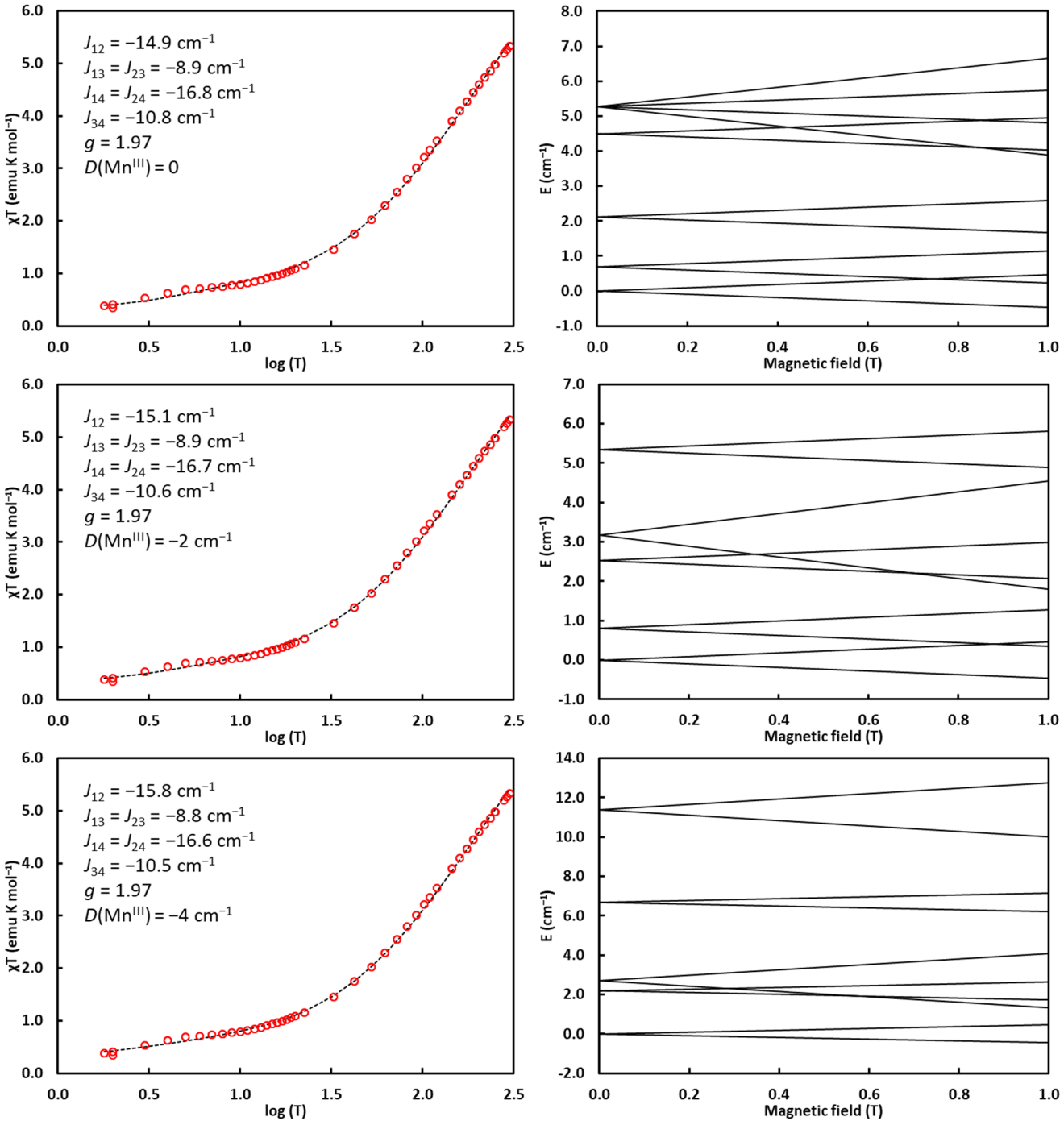

Figure S15. Fit parameters and corresponding χT vs. log(T) plots and Zeeman splitting diagrams for **3-ox**.

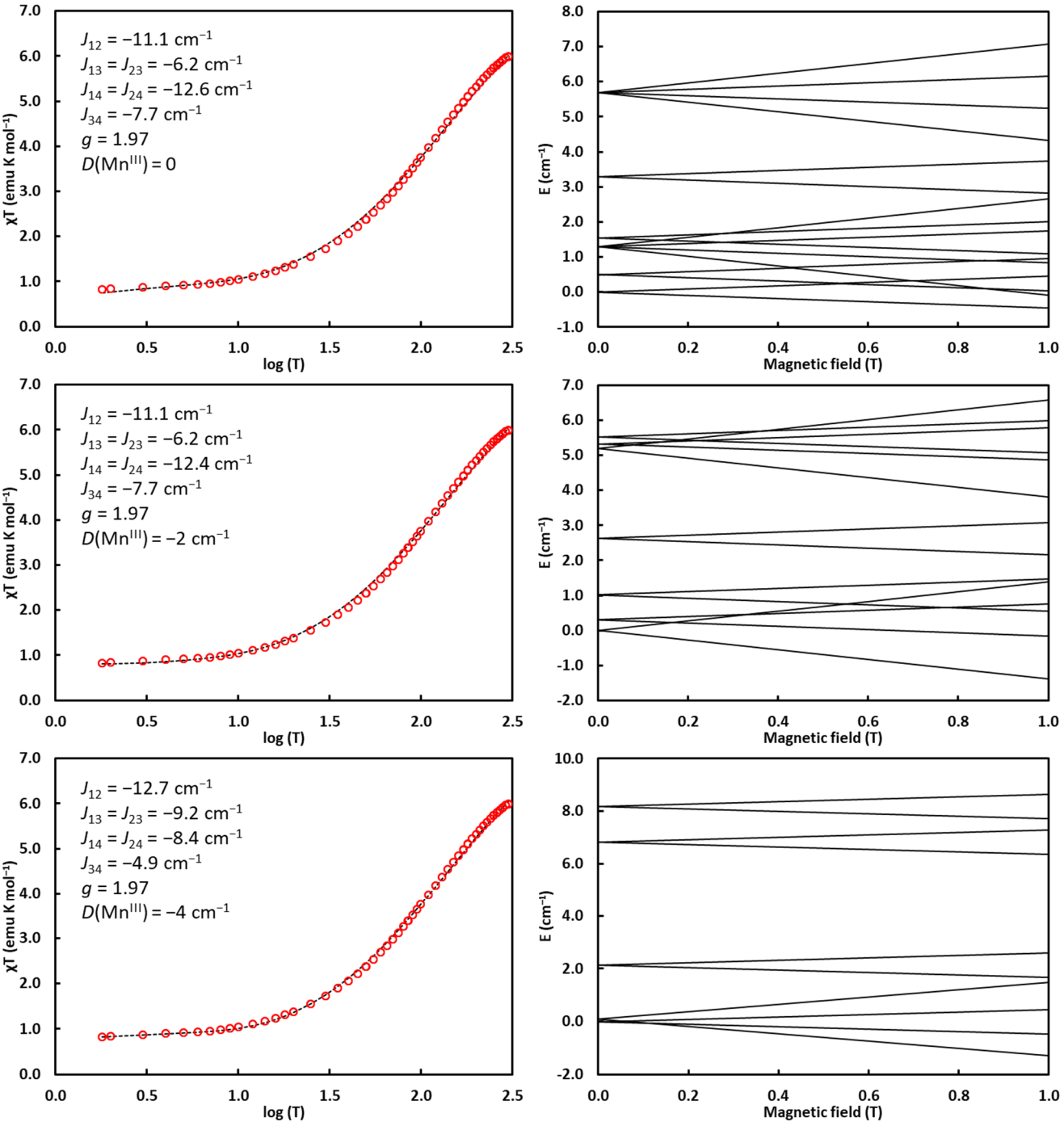

Figure S16. Fit parameters and corresponding χT vs. log(T) plots and Zeeman splitting diagrams for **4-ox**.

EPR spectroscopy

Samples were prepared as solutions (*c.a.* 1 mM) in 1:1 CH_2Cl_2:2-MeTHF and rapidly cooled in liquid nitrogen to form a frozen glass. All X-band CW-EPR and Q-band pulse EPR/ENDOR experiments presented in this study were acquired at the Caltech EPR facility, while D-band (130 GHz) pulse experiments were performed at the CalEPR facility in the Britt lab at the University of California, Davis. X-band CW EPR spectra were acquired on a Bruker (Billerica, MA) EMX spectrometer using Bruker Win-EPR software (ver. 3.0). Temperature control was achieved using liquid helium and an Oxford Instruments (Oxford, UK) ESR-900 cryogen flow cryostat and an ITC-503 temperature controller. Pulse EPR and electron nuclear double resonance (ENDOR) experiments were acquired using a Bruker ELEXSYS E580 pulse EPR spectrometer using a Bruker D2 pulse ENDOR resonator for Q-band experiments. Temperature control was achieved using an Oxford Instruments CF-935 helium flow cryostat and a Mercury ITC temperature controller. Spectra were simulated using EasySpin[5] (release 5.2.16) with Matlab R2017a.

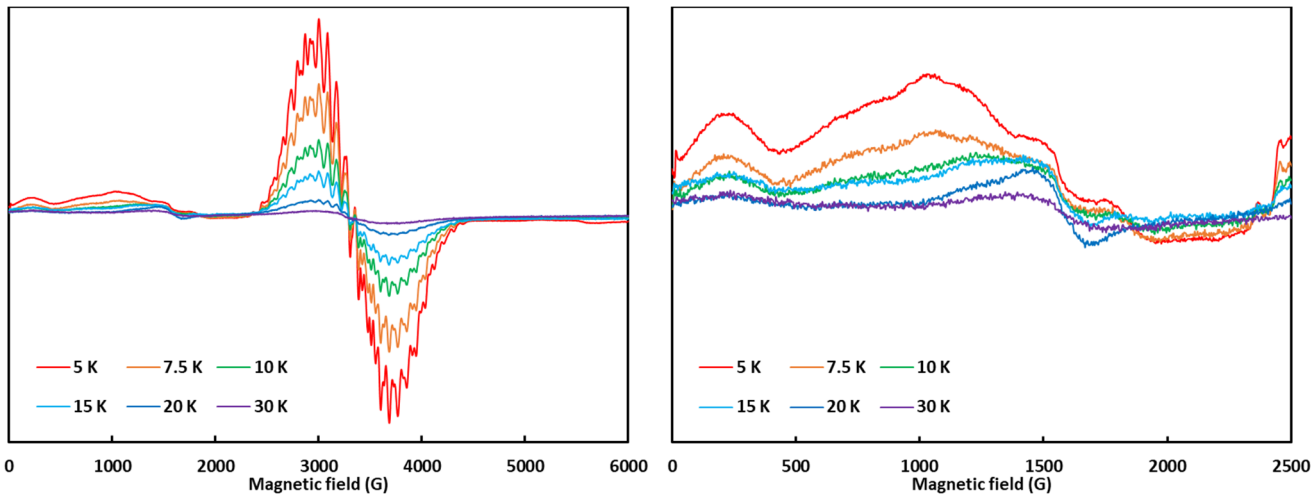

Figure S17. Temperature-dependent X-band CW-EPR spectra of a freeze-quenched reaction mixture of **1** and $[(4\text{-BrPh})_3N][SbCl_6]$. Data acquisition parameters: frequency = 9.35 MHz, power = 2 mW, conversion time = 20.48 ms, modulation amplitude = 8 G.

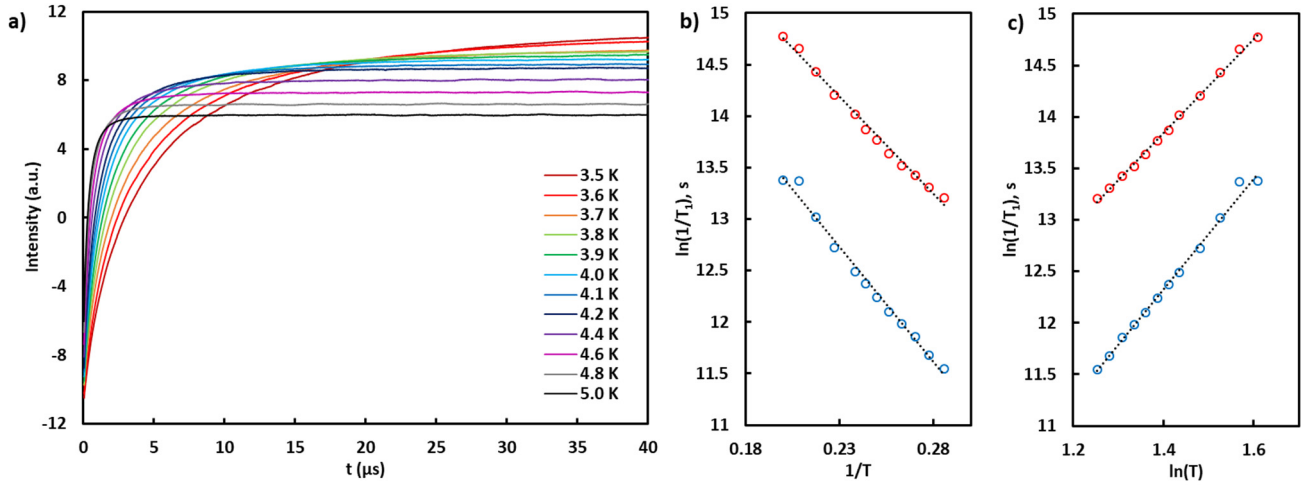

Figure S18. a) Temperature-dependent inversion recovery trace for **3-ox**. b) Plot of $\ln(1/T_1)$, T_1 in seconds vs. 1/T (K^{-1}) for the fast and slow exponential components. Slope of the linear fit: 18.9 K (red), and 22.4 K (blue). c) Plot of $\ln(1/T_1)$ vs. ln(T) and linear fit to the data. Acquisition parameters: frequency = 34.07 MHz, π_{MW} = 24 ns, τ = 140 ns, srt = 2 ms.

All D-band pulsed EPR spectroscopic studies were performed at a temperature of 5.2 K using a recently redesigned home-built 130 GHz EPR spectrometer equipped with an Oxford Instruments CF-935 liquid helium cryostat and an ITC-503 temperature controller.[6] The spectrometer is equipped with an 8 T cryogen-free magnet (Cryogenic Limited, UK). All data were acquired using a TE011 mode cylindrical resonant cavity designed and manufactured by HF EPR Instruments, Inc. (V. Krymov, New York).[7] Spectrometer control is achieved using the SpecMan software.[8] ESE-EPR and electron-electron double resonance-detected NMR (EDNMR) of **3-ox** were recorded at D-band (130 GHz). ESE-EPR spectra were recorded using a Hahn-echo sequence, $\pi/2$-τ-π-τ-echo and EDNMR spectra were recorded using the sequence π_{HTA}-T- $\pi/2$-τ-π-τ-echo. Pulse parameters are as follows, ESE-EPR: π_{MW} = 90 ns, τ = 300 ns, Temperature = 5.2 K; EDNMR: HTA = 5 μs, T = 5 μs, π_{MW} = 80 ns, τ = 300 ns, Temperature = 5.2 K, 2 MHz resolution. The EDNMR in Figure S19 is a subtraction of the experimental data in Figure S20 with a Lorentzian and Gaussian to model the central blind spot as in Cox et al.[9] The resulting spectrum is inverted and the right-hand side is what is plotted in Figure S19. A comparison of the right-hand side and left-hand side is shown in Figure S21.

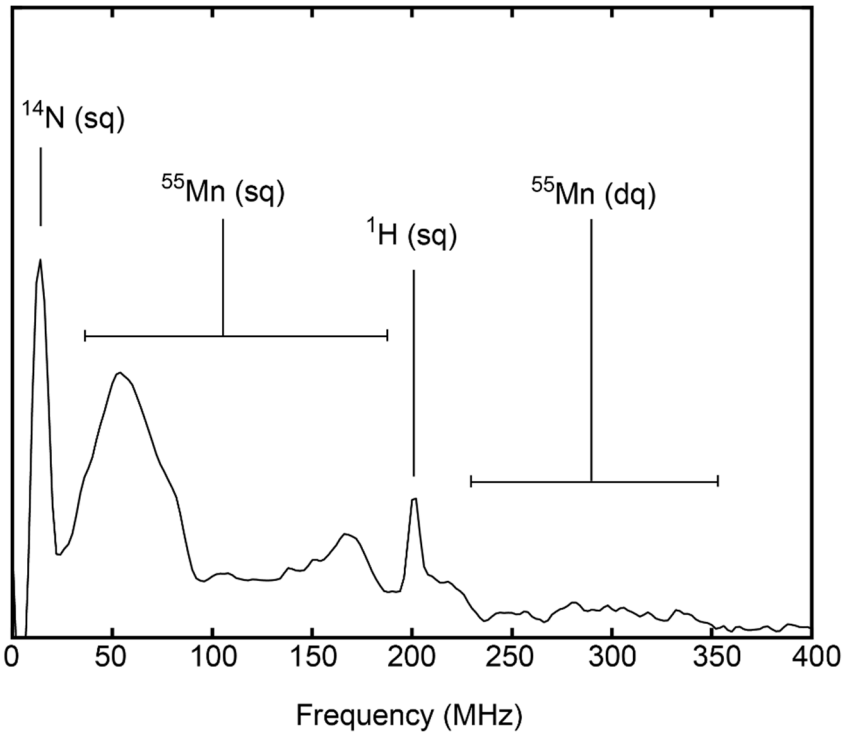

Figure S19. D-band EDNMR of **3-ox** recorded at 4.7 T.

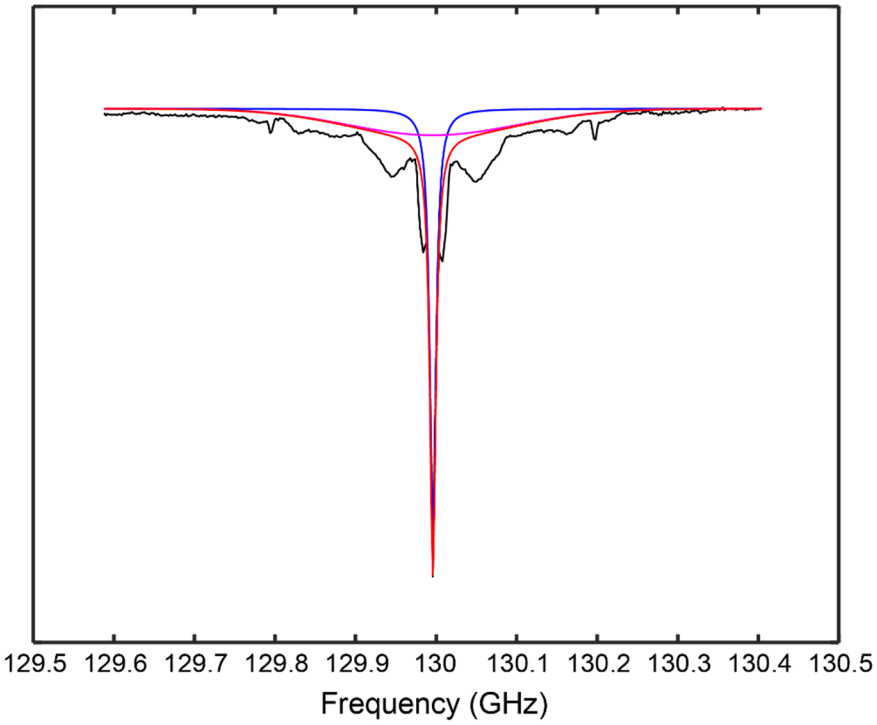

Figure S20. EDNMR spectrum of **3-ox** (black trace). The blind spot was modeled as the sum (red trace) of a Lorentzian (blue trace) and a Gaussian (magenta trace) centered about the resonator frequency 129.996 GHz.

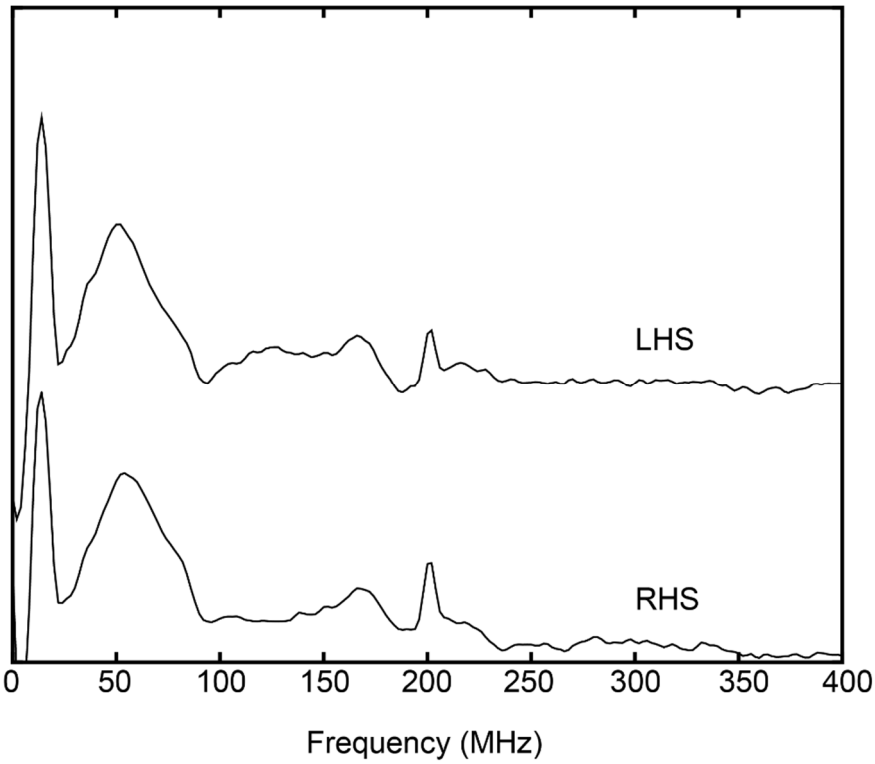

Figure S21. Comparison of the right-hand side (RHS) and left-hand side (LHS) from Figure Y after Lorentzian subtraction.

References

(1) Reed, C. J.; Agapie, T., *Inorganic Chemistry* **2017,** *56*, 13360.
(2) Ravel, B.; Newville, M., *Journal of Synchrotron Radiation* **2005,** *12*, 537.
(3) Zabinsky, S. I.; Rehr, J. J.; Ankudinov, A.; Albers, R. C.; Eller, M. J., *Physical Review B* **1995,** *52*, 2995.
(4) Chilton, N. F.; Anderson, R. P.; Turner, L. D.; Soncini, A.; Murray, K. S., *Journal of Computational Chemistry* **2013,** *34*, 1164.
(5) Stoll, S.; Schweiger, A., *Journal of Magnetic Resonance* **2006,** *178*, 42.
(6) Oyala, P. H.; Ravichandran, K. R.; Funk, M. A.; Stucky, P. A.; Stich, T. A.; Drennan, C. L.; Britt, R. D.; Stubbe, J., *Journal of the American Chemical Society* **2016,** *138*, 7951.
(7) Dorlet, P.; Seibold, S. A.; Babcock, G. T.; Gerfen, G. J.; Smith, W. L.; Tsai, A.-l.; Un, S., *Biochemistry* **2002,** *41*, 6107.
(8) Epel, B.; Gromov, I.; Stoll, S.; Schweiger, A.; Goldfarb, D., *Concepts in Magnetic Resonance Part B-Magnetic Resonance Engineering* **2005,** *26B*, 36.
(9) Cox, N.; Lubitz, W.; Savitsky, A., *Molecular Physics* **2013,** *111*, 2788.